Design of a Compact Multi-band Circularly Polarized Antenna for Global Navigation Satellite Systems and 5G/B5G Applications

Oluyemi P. Falade, Masood Ur-Rehman, Xiaodong Yang, Ghazanfar Ali Safdar, Clive G. Parini and Xiaodong Chen

Oluyemi P. Falade, Clive Parini and Xiaodong Chen
School of Electronic Engineering & Computer Science, Queen Mary, University of London, Mile End, London UK (e-mail: oluyemifalade@gmail.com).

Masood Ur-Rehman
James Watt School of Engineering, University of Glasgow, University Avenue, Glasgow, UK (e-mail: masood.urrehman@galsgow.ac.uk).

Xiaodong Yang
School of Electronic Engineering, Xidian University, Xi'an, Shaanxi, China, 710071 (email: xdyang@xidian.edu.cn).

Ghazanfar Ali Safdar
School of Computer Science & Technology, University of Bedfordshire, University Square, Luton, UK (e-mail: ghazanfar.safdar@beds.ac.uk).

Corresponding authors: Oluyemi P. Falade and Masood Ur-Rehman.

***Abstract*— Design of a multi-band circularly polarized antenna is proposed in this paper. The antenna has a simple and compact form factor by employing single feed stacked patch structure. It exhibits good performance at the GNSS frequency bands of L1, L2 and L5 and cellular communications frequency band of 2.3 GHz. The antenna has a 3-dB axial ratio bandwidth of 1.1%, 1.0%, 4.1% and 1.5% at the four operating bands of L1 (1.575 GHz), L2 (1.227 GHz), L5 (1.176 GHz) and 2.3 GHz. The antenna also achieves a gain of more than 2.2 dBiC and efficiency of more than 70% at the four frequencies. A detailed parametric study is carried out to investigate the importance of different structural elements on the antenna performance. Results are verified through close agreement of simulations and experimental measurements of the fabricated prototype. Good impedance matching, axial ratio bandwidth and radiation characteristics at the four operating bands along with small profile and mechanically stable structure make this antenna a good candidate for current and future GNSS devices, mobile terminals and small satellites for 5G/Beyond 5G (5G/B5G) applications.**

***Keywords*— Stacked patch, Circular polarization, Global Navigation Satellite Systems, 5G/B5G, Multi-band, Symmetric slots.**

I. Introduction

The wireless technology is experiencing rapid advances due to advent of innovative hardware as well as software techniques. Availability of wide variety of applications along with continuous component miniaturization demands simple, compact and cost effective but optimally performing antennas. Satellites, navigation devices and mobile terminals are also following these treads to improve performance and economic viability.

Microstrip antennas serve as the preferred choice for the commercial applications due to their inherent features of reduced complexity, ease of integration and cost effectiveness [1-6]. Global Navigation Satellite Systems (GNSSs) are now part of majority of the communication devices. Circularly polarized (CP) antennas are preferred choice for the GNSSs as they have the ability to effectively reduce the Faraday's rotation effect in the ionosphere; require no strict orientation match between transmitting and receiving antennas; and combat the multipath effect [7-12]. Provision of multiple services in a single and small communication device is another commercial preference to increase customer interest. Majority of these services require more than one antenna to cover several frequency bands that makes the device size quite large and give rise to mutual coupling if each band is served by a single antenna. This challenging task has compelled the antenna engineers to look for new solutions by redesigning and transforming the known antenna types. A single feed and compact multi-band CP antenna that can perform multiple functions effectively and simultaneously is reckoned as a good alternative to overcome these space and performance limitations [8, 13]. This multi-function/multi-band antenna solution will not only leave space for extra components and cut the cost but also improve operation due to reduced weight and mutual coupling for small satellites or handheld mobile terminals.

Multi-band antennas have attracted interest of researchers worldwide. A number of studies have discussed multi-band circularly polarized and/or linearly polarized (LP) antenna designs with single or multiple feeding points in the open literature [14-32]. Quadrifiler helixes, annular rings, slotted patches, Split Ring Resonators (SRRs) and stacked patches are some of the popular ways to generate multiple resonances with good CP operation.

A dual band quadrifilar helix antenna operating at L1/L2 or L1/L5 bands has been discussed in [14]. The antenna employs a folded meander line structure on a cylindrical dielectric. A dual-band antenna using cavity-backed annular slot structure has been presented by Hsieh et al. [15]. The antenna operates at L1 and L2 bands with a low gain of 1.45 dBiC. Hoang *et al.* have presented a quad-band CP antenna at S- and C- band [16]. The antenna configuration has a patch composed of an inverted U-shaped with additional I-shaped and L-shaped strips all rotated by 45^0. To convert LP to CP, a frequency selective surface is used. Nasimudden *et al.* have proposed a single band CP antenna working at L1 band utilizing four square-ring slots cut on a square patch and grounding the central patches through metallic vias [17]. Ali *et al.* have proposed a microstrip-fed slotted-patch antenna having a kite-shaped slot in the radiating patch to obtain miniaturization, C- and G-shaped slots in the ground plane to incorporate multiband operation. A 36% reduction in volume of the proposed design is achieved with operation at 3.6 GHz, 5.8 GHz, 6.9 GHz and 9.5 GHz bands [18]. A tri-band microstrip patch antenna using FR-4 substrate employing an open loop

resonator, a split rectangular slot and a stub at the non-radiating edge for multi-band GPS operation at L1, L2 and L5 bands is presented by Supriya et. al [19]. The antenna has a narrowband operation with gains of 4.03 dBi, 5.6 dBi and 2.31 dBi at the three frequency bands. Four unequal circular patches are assimilated on the corners of a square patch radiator to design an L1 band CP antenna in [20].

A triband antenna composed of a tri-mode monopole, an open-slot etched on the ground, and a parasitic strip is proposed in [21]. The antenna resonates at 0.9, 1.85, and 2.4 GHz but offers offers an impedance matching of −6 dB. Fady et. al have proposed a multiband antenna consisting of a planar dipole with four arms. Though the antenna resonates at 1.6 GHz, 2.0 GHz, 3.5 GHz, 4.0 GHz and 5.8 GHz frequencies, it requires a large form factor of 37 mm × 67 mm [22].

A single feed hexa-band antenna for WLAN/Wi-MAX/SDARS and C-band applications has been designed by Alam *et al.* in [23]. The antenna uses a monopole structure with on the partial ground plane having a total volume of $47 \times 40 \times 1.57\,\text{mm}^3$. Split ring resonator (SRR) loading has been used to achieve multiple circularly polarized bands. SRR loading technique has also been used in [24] along with a truncated slot structure and coplanar waveguide (CPW) feed to realise a triband CP antenna. The antenna resonates at 4.15 GHz, 4.77 GHz and 5.1 GHz.

Stacked patch structures are popular in multiband antennas as it provides more control on the radiation characteristics of individual operating bands where each patch supports one or the other operating band. Moreover, it offers enhanced impedance, higher axial ratio bandwidth, CP purity and better gain as compared to traditional patch radiators [25-37]. A dual band L1 and L2 CP operation has been achieved by placing two asymmetric slit square patches and a cross-shaped slotted square patch over a reactive impedance surface in [25]. This design is modified to exhibit triple-band operation at L1, L2 and L5 bands in [26] by using three stacked patches with two different pairs of symmetric slits, four different sized symmetric cross-shaped slots and truncated corners over reactive impedance surface.

Quad-band CP/LP stacked patch antennas have been presented in [27-28]. A not so preferred 6-dB axial ratio has been used in [27] while an air gap of 5 mm is used to broaden the bandwidth in [28]. A two-layer stacked circular patch antenna for dual-band operation at L1 and L2 bands is proposed by Du Li *et al.* [29]. A complex capacitive coupled feeding network of four ports with equal magnitude and 90^o phase shift feeds the antenna. The antenna does not exhibit a clear distinction between the two bands however, as the reflection coefficient response is below -14 dB throughout, making it essentially a broadband antenna.

Jianxing Li *et al.* have suggested a stacked annular patch design for multiband operation at 1583 MHz, 2492, 1616 MHz and 1268 MHz bands to support L1 and BDS-1/2 (for Chinese COMPASS navigation system) [30]. The antenna employs four stacked annular patches and a stepped-radius shorting pillar fed by a quadrature phase feed network comprising of four 90^o stripline baluns. A clear separation of the four bands is missing in this design as well. Performance of two CP single- and dual-feed stacked patches incorporating a high and low dielectric constant material combination is analysed by Waterhouse [31]. It is shown that a 10-dB return-loss bandwidths in excess of 25% and lower cross-polarization can be achieved with these configurations.

A LP antenna for tri-band operation at GSM 900/1800 and GPS L1 frequencies is discussed in [32]. The antenna employs a complex configuration by stacking a

microstrip square ring patch with truncated corners and two nested small loops fed by a multistage matching network of lumped components and shorting pins.

A dual-band stacked patch 2 × 3 antenna array having single elements composed of two square ring patches in two different thicknesses of dielectric substrates is presented in [33]. The antenna array works at L1 and L2 frequency bands. The feeding network has used six hybrid couplers. A stacked patch antenna design having square patches with semicircular cutouts connected physically rather than parasitically is discussed in [34]. The antenna provides 100% bandwidth from 23.9 to 72.2 GHz. An inkjet-printed flexible stacked patch antenna covering 4.7-5 GHz frequencies is presented by Li *et al.* [35]. The antenna consists of two layers of patches, where the first layer is printed on a Kapton polyimide substrate, which is then covered, by an SU-8 polymer and a Minkowski fractal geometry patch on the top as the second layer.

A triple-band stacked patch CP antenna covering L1, L2 and BDS-1 bands has been investigated in [36]. A four L-probe feeding network excites the antenna while two shorted annular rings formed with a circular array of metallic vias is used to suppress the mutual coupling between the patches. These designs are both complex and hard to integrate or carry large size that makes them unsuitable for compact terminals. Others have used complex feeding techniques. The use of air substrate compromises the rigidity of the antenna. Moreover, the distinction of individual frequency bands is not always visible which introduces unwanted noise across the broadband. Therefore, research for a new multi-band antenna design rectifying these issues is necessary to satisfy needs of increasingly demanding wireless communication and navigation market supporting 5G (5G/B5G) applications.

This paper proposes a compact, single feed stacked patch, multi-band, CP antenna for GNSS and 2.3 GHz frequency bands operation to fulfill this gap. The proposed antenna exhibits good distinction between different frequency bands with good impedance bandwidth and axial ratio. The minimum axial ratio and the resonant frequency of the impedance bandwidth also coincide which is a challenge in CP antenna. Simplicity, compactness and ease of integration of this design make it suitable for mobile terminals, GPS receivers and small satellites. Following the introduction, the rest of the paper is organized in four sections. Overview of the proposed antenna design with geometrical details is given in Section II. Section III presents the simulated and measurement results along with analysis of the antenna performance. Section IV carries out a detailed parametric investigation to highlight impact of key structural elements on the antenna performance. Comparison of the proposed antenna with state-of-the-art is carried out in Section V while conclusions are drawn in Section VI.

II. Antenna Design

The proposed multi-band CP antenna utilizes a stacked-patch structure as shown in Fig. 1. It consists of four layers of radiating patches and substrates stacked on top of each other and a ground plane at the bottom. The lower patch layer is printed on Roger's R04003 substrate (having a thickness of 1.524 mm, relative permittivity of 3.38 and loss tangent of 0.0027) while the three upper layers employ FR4 substrates (with thickness of 1.6 mm, relative permittivity of 4.4 and loss tangent of 0.02). The four radiating patches support antenna operation at the four required bands. The lower patch is used to generate the GPS L5 band (Band 1); middle patch produces GPS L2 band (Band 2); upper patch makes the antenna to resonate at the GPS L1 band (Band

3) and the topmost patch produces resonance at 2.3 GHz (Band 4) for 5G (5G/B5G) applications.

Among the GNSS frequencies, L1 and L5 bands are common to most of the GNSSs including GPS (USA, world's most utilized satellite navigation system), Galileo (Europe), BeiDou (China) and QZSS (Japan) while L2 band is GPS specific but can be easily replaced with any other frequency bands for other GNSSs [7]. The proposed antenna is suitable for the L1 (GPS), G1 (Glonass), B1 and B1-2 (BeiDou) bands on top of L5 and L2 frequencies.

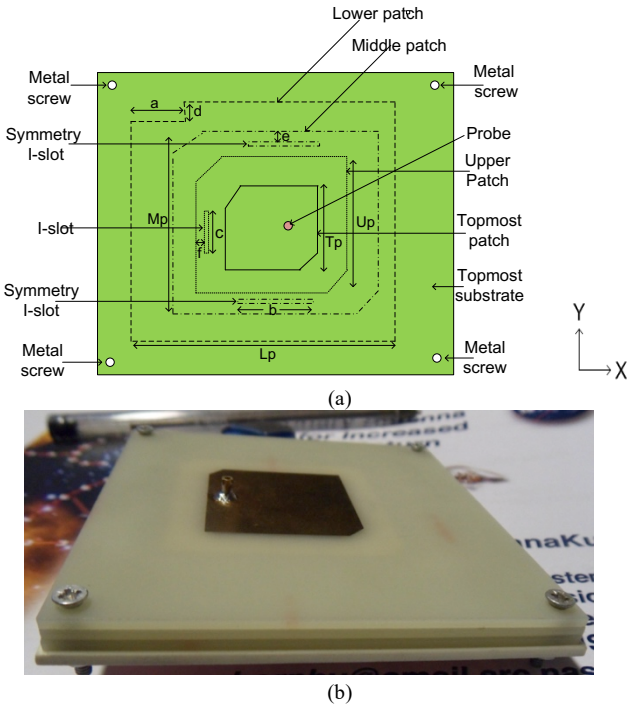

Fig. 1: Geometry of the proposed stacked patch multi-band CP antenna (a) Top view (b) Fabricated prototype.

Total volume of the proposed antenna is 0.26 $\lambda_0 \times 0.26\ \lambda_0 \times 0.024\ \lambda_0$ where λ_0 is the wavelength at GPS L5 band. The lengths of the lower, middle, upper and topmost patches are Lp = 65.4 mm, Mp = 55.8 mm, Up = 42.9 mm and Tp = 30.0 mm, respectively. Ground plane size is 80 mm x 80 mm. The antenna is excited by a single 50 Ω coaxial probe feed connected to the topmost patch through via-holes in the lower patches. These via-holes reduce the inductance caused by the probe by improving the capacitive effect. The excitation of the subsequent patches is through electromagnetic coupling. Symmetry I-slots are etched on the middle and upper patches to achieve an AR below 3 dB. This also results in coinciding the minimum axial ratio with the resonant frequency of each band. Dimensions of the I-slot in the middle patch is b = 10 mm × 1 mm at e = 6.9 mm while that of the I-slot in the upper patch is c = 8 mm × 1 mm at f = 1.45 mm.

A dual orthogonal degenerated mode is introduced at the lower patch through the slit cut while the current path on other patches is perturbed through corner truncations to achieve circular polarizations. Four metal screws are used at the four corners of the antenna to prevent air gap and enhance a firm grip. This arrangement also makes it easy to attach the antenna to other components and platforms. Each screw has a diameter of 2.5 mm and a length of 7.5 mm. The fabricated prototype of the proposed antenna is shown in Fig. 1 (b).

III. Results and Discussion

The antenna is modeled, simulated and optimized numerically using Computer Simulation Technology (CST) Microwave Studio [37]. In order to validate the numerical analysis, a prototype of the optimized antenna design is fabricated and tested. The prototype measurements are performed at the Antenna Measurement Laboratory of Queen Mary University of London. The antenna performance is analyzed in terms of reflection coefficient, bandwidth, axial ratio and radiation patterns at the four operating bands.

TABLE I: SUMMARY OF THE MEASURED AND SIMULATED REFLECTION COEFFICIENT OF THE MULTI-BAND CP ANTENNA.

Operating band	Frequency range (GHz)	Bandwidth (MHz)	Bandwidth % at resonant frequency
Simulated GPS L5	1.163-1.180	17	1.4
Measured GPS L5	1.153-1.166	13	1.38
Simulated GPS L2	1.212-1.237	25	2.0
Measure GPS L2	1.215-1.242	27	2.2
Simulated GPS L1	1.559-1.596	37	2.3
Measured GPS L1	1.566-1.606	40	2.5
Simulated 2.3GHz	2.277-2.331	54	2.3
Measured 2.3GHz	2.254-2.316	62	2.7

The measured and simulated reflection coefficient responses are plotted and compared in Fig. 2. The impedance bandwidths of the antenna at the four operating bands are summarized in Table I. A good agreement between the measured and simulated results can be observed. Slight discrepancies are associated to the fabrication imperfections. The antenna exhibits good bandwidth sufficient for the GPS and LTE operation at the four frequency bands as the required bandwidths at the four bands are 2.046 MHz for Standard Positioning Service (commercial use) and 20.46 MHz for Precise Positioning Service (military use) at L1 band, 20.46 MHz at L2; 20.46MHz at L5 and ±5MHz at the uplink at 2.3 GHz band [7,8,38,39]. Maximum bandwidth of 2.7% is being observed at Band 4 while a minimum of 1.1% is being observed at GPS L5.

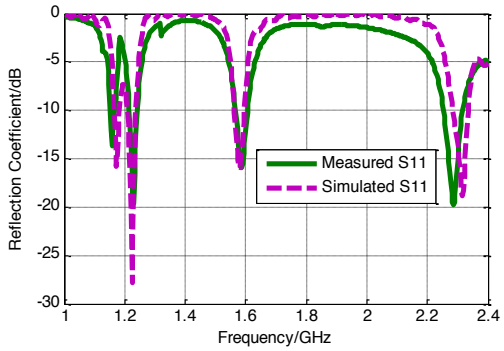

Fig. 2: Measured and simulated reflection coefficient response of the proposed multi-band CP antenna.

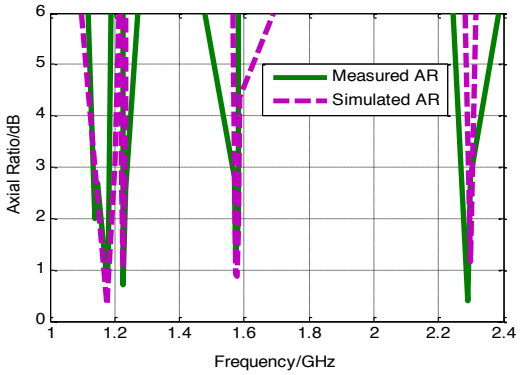

Fig. 3: Measured and simulated axial ratio of the proposed multi-band CP antenna.

The measured and simulated axial ratio (AR) curves are presented in Fig. 3. The measured 3-dB axial ratio bandwidth is noted to be 4.1 % at GPS L5 frequency band; 1.0 % at GPS L2 frequency band; 1.1 % at GPS L1 frequency band and 1.5 % at the 2.3 GHz frequency band. These values are in close agreement to the simulated axial ratio bandwidths of 5.3 % at GPS L5 band; 0.7% at GPS L2 band; 0.8% at GPS L1 band and 0.5% at the 2.3 GHz band. A wider axial ratio bandwidth at the GPS L5 band is due to the presence of two different dielectric substrates [23-24]. Thickness of the substrate is also a contributing factor towards it, which increases the surface wave efficiency and thus, improving the axial ratio bandwidth in this frequency band.

Surface current distributions illustrated in Fig. 4 further elaborate it by portraying the function of each of the patches independently. Fig. 4(a) depicts a stronger current generation on the ground plane and the lower patch as compared to the middle, upper and topmost patches. It can be deduced from this result that the tuning of the lower patch affects GPS L5 band and does not influence the operation at other frequency bands. Similarly, Fig. 4(b) illustrates the current distribution of the antenna at GPS L2 band. A high current distribution can be observed on the middle patch and the edges of the upper patch while currents on the lower and topmost patches are very weak. It shows that the working of the antenna at GPS L2 band is dictated primarily by the middle patch only. Similar trend is observed in Figs. 4(c) and (d) which show the current distribution at GPS L1 and 2.3 GHz bands. It can be deduced that the size of each patch is important to the resonant frequency. Also, the size of the patches must decrease as the frequency increases for stacked patch technique to be effective.

The measured and simulated circularly polarized radiation patterns of the multi-band antenna at GPS L5 and L1 frequency bands in XZ-plane are compared in Fig. 5. The measurements have been performed in an anechoic chamber and circular polarized patterns are established using the amplitude-phase method [4]. A good agreement between the measured and simulated results is found. The results show that the right-hand circular polarization (RHCP) is stronger than the left-hand circular polarization (LHCP) by about 15 dB at the broadside. A similar trend is being observed at the other operating frequencies (results for other bands are not included to maintain brevity. Small discrepancies in the measured and simulated results are due to the coaxial cable loss and fabrication tolerances. This as well as the closeness of the ground plane to the lower patch has led to a relatively poor front-to-back ratio of the radiation patterns.

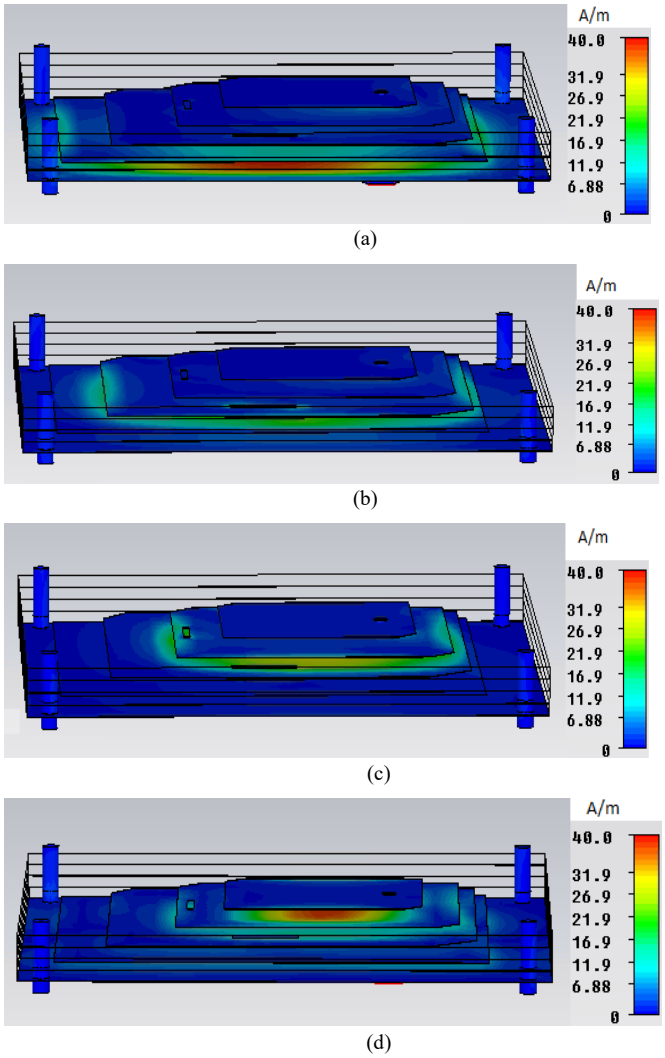

Fig. 4: Surface current distribution of the proposed multi-band CP antenna at, (a) GPS L5 band, (b) GPS L2 band, (c) GPS L1 band and (d) 2.3 GHz band.

The beamwidth of a GNSS antenna observed in the upper hemisphere is a measure of receiver's satellite visibility. A good beamwidth assures that the receiver is able to acquire positioning signals from at least four satellites within its view to correctly identify its position. The radiation patterns in Fig. 5 show that that antenna achieves a broad 3-dB axial ratio beamwidth at GPS L5, L2 and L1 frequency bands. The beamwidths are observed to be excellent as 170^0, 150^0, and 180^0, respectively. The 3-dB axial ratio beamwidth appears to be 40^0 at 2.3 GHz band. Measured values of gain are very good with values of 2.23, 2.91, 3.40 and 2.70 dBiC at the four frequency bands, respectively. The antenna also offers good efficiency of 70%, 75%, 77% and 72%, respectively at the four operating frequencies.

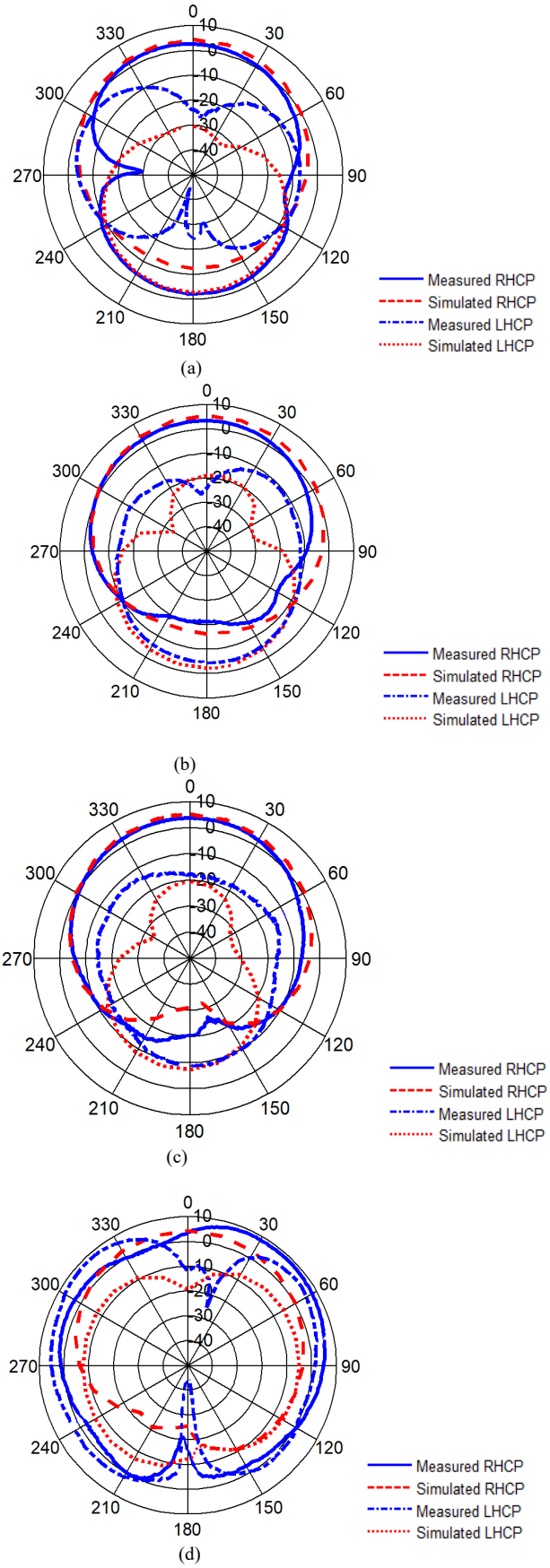

Fig. 5: Measured and simulated RHCP and LHCP radiation patterns of the proposed multi-band antenna in XZ plane at, (a) GPS L5 band, (b) GPS L2 band, (c) GPS L1 band and (d) 2.3 GHz band.

IV. Analysis of Design Parameters

The resonance frequency of the proposed quad-band antenna at each of the bands of operation is primarily dependent on the size of the corresponding radiating patch. Also, the lower patch acts as a ground plane to each of the subsequent upper patches. Impact of these key design parameters on the resonance frequency and axial ratio are studied in this section.

A. Length of Topmost Patch (Tp)

Fig. 6 plots the simulated reflection coefficient and AR with different lengths of the topmost patch *(Tp)* keeping dimensions of other structural parameters fixed. It can be observed that the reflection coefficient response remains indifferent for GPS L5, L2 and L1 frequency bands. However, a significantly large variation takes place at 2.3 GHz frequency band. As the *Tp* increases, the resonance frequency at 2.3 GHz band decreases. It is due to the fact that increase in the patch length has lengthened the current path of the antenna that in turn, lowers the resonance frequency.

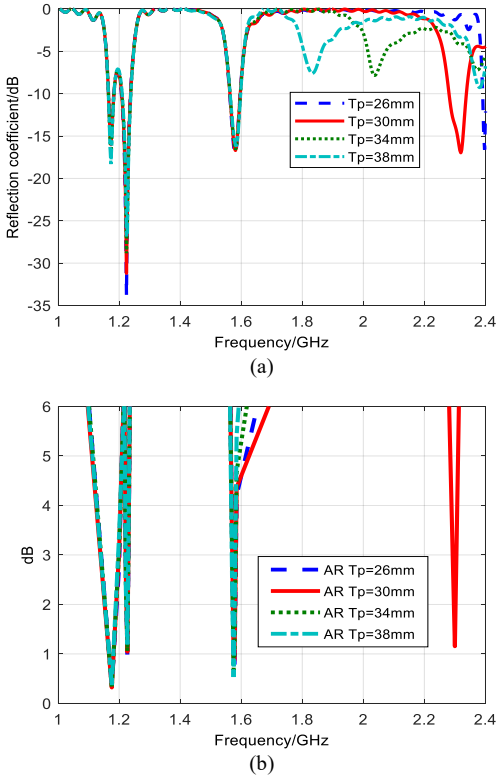

Fig. 6: Effects of length of the topmost patch *(Tp)* on the performance of the proposed antenna, (a) Reflection coefficient response, (b) Axial ratio.

Fig. 6(b) shows that the axial ratio at the 2.3 GHz band is significantly affected due to variation in *Tp* and only have an acceptable value at *Tp* = 30 mm. It is also evident from this study that the resonance frequency for 2.3 GHz operation can be controlled independently by adjusting the length of the topmost patch without affecting the performance at other frequency bands.

B. Length of Middle Patch (Mp)

Fig. 7 analyses the effects of varying lengths of the middle patch *(Mp)* on the antenna performance. It can be observed that antenna operation at GPS L2 band bears the burden of any changes in the dimension of the middle patch. It is due to the fact

that increase in *Mp* lengthens the surface current path resulting in decreasing the resonance frequency of GPS L2 band. As *Mp* increases, the resonant frequency of GPS L1 band remains unchanged until at *Mp* = 57.8 mm where GPS L5 and GPS L2 bands collide. The reason for this is that, the resonance frequency of GPS L2 at this length is closer to that of GPS L5. The axial ratio at GPS L5 improves as *Mp* increases until it reaches to *Mp* = 57.8 mm where it exhibits an opposite trend. As *Mp* increases, the resonant frequency of GPS L2 decreases. There is a profound effect when *Mp* = 47.8 mm which causes a shift in the resonance frequency of GPS L1.

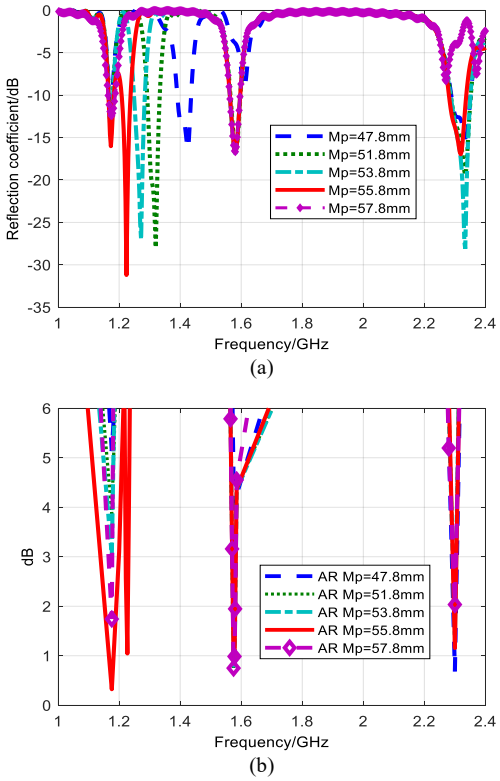

Fig. 7: Effects of length of middle patch (*Mp*) on the antenna performance, (a) Reflection coefficient response, (b) Axial ratio.

This is a result of the reduction in the size of the middle patch beyond the acceptable value, which serves as a ground plane to the upper patch. More so, when *Mp* = 57.8 mm, a notch appears at 2.3 GHz leading to effectively a dual band operation around this frequency. It can be deduced from this observation that below *Mp* = 57.8 mm, these two bands overlap resulting in a wider band of 62 MHz at 2.3 GHz frequency. The axial ratio at GPS L2 becomes poor as the *Mp* increases until *Mp* = 55.8mm where a better axial ratio is achieved. The length, *Mp,* has no significant effect on the reflection coefficient and axial ratio of GPS L1 and 2.3 GHz band operation.

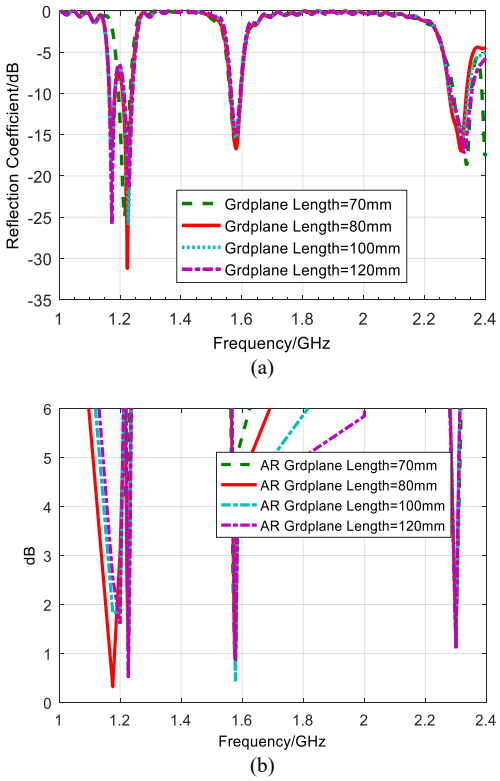

Fig. 8: Effects of varying length of ground plane on the antenna performance (a) reflection coefficient and (b) axial ratio.

C. Length of Ground Plane

The ground plane size also affects the antenna performance as shown in Fig. 8. As the ground plane length increases, the impedance matching improves. More so, a better cross polarization is achieved by having a larger ground plane. When the ground plane size is reduced to 70 mm, a single wide-band covering operating at GPS L5 and L2 is observed. Furthermore, the ground plane size has a significant effect on the interaction between the surface current from the ground plane and the lower patch but does not impact the working of other patches. From the simulation result, it can be observed that the gain and efficiency increase as the ground plane increases.

D. Effect of Metal Screws

No significant effect on the reflection coefficient and axial ratio of the proposed antenna has been observed with or without metal screws.

TABLE II
COMPARISON BETWEEN THE PROPOSED ANTENNA AND STATE-OF-THE-ART MULTIBAND GNSS ANTENNAS.

Ref.	Antenna structure	Electrical Size	Operating Bands	10-dB Bandwidth (%)	3-dB AR Bandwidth (%)	3-dB AR Beamwidth (Degrees)	CP Gain (dBiC)
[17]	Single-feed stacked patches with non-symmetric slots on a metamaterial reactive impedance surface	0.32 λ_o × 0.32 λ_o × 0.024 λ_o @ 1.2 GHz	L1 L2 L5	5.16 3.68 1.45	3.19 3.04 2.21	120°	5.53 3.25 2.88
[24]	Stacked patch quad-electromagnetic coupling with air substrate	0.570 λ_o × 0.57 λ_o × 0.001 λ_o @ 915 MHz	915 MHz 2.45 GHz	5.05 8.16	0.90 1.60	Not reported	8.00 2.50
[25]	Stacked circular patches fed by a four-port feed network	0.64 λ_o × 0.07 λ_o @ 1.2 GHz	L1+L2	44.0	31.5	128°	3.00
[26]	Stacked annular patches with stepped radius shorting pillar fed by quadrature phase baluns	0.28 λ_o × 0.048 λ_o @ 1.2 GHz	1.268 GHz L1 1.616 GHz 2.482 GHz	15.77 12.63 12.38 8.10	0.78 6.31 0.62 0.8	Not reported	2.14 2.74 3.42 5.43
[32]	Stacked circular patches with annular shorting vias fed by four L-probes	0.68 λ_o × 0.68 λ_o × 0.098 λ_o @ 1.2 GHz	L1 L2 2.482 GHz	14.2 9.47 5.62	Not reported	Not reported	6.50 6.25 6.00
This work	Stacked patch with slit and symmetry I-slot	0.26 λ_0 × 0.26 λ_0 × 0.024 λ_0 @ 1.2 GHz	L1 L2 L5 2.3 GHz	2.50 2.20 1.38 2.70	1.10 1.00 4.10 1.50	180° 150° 170° 40°	3.40 2.91 2.23 2.70

V. Comparison with State-of-the-art Multiband GNSS Antennas

The proposed antenna design is compared with related stacked patch antennas reported in open literature [17], [24-26], [32] in terms of structure, size and radiation characteristics to show its novelty and effectiveness. Table II summarizes the key comparison parameters for these antennas.

It is evident from this comparison that the proposed antenna exhibits wider angular coverage than rest of the compared designs except [25] which is in essence a broadband antenna that shows no distinction between the L1 and L2 bands despite claiming to be a dual-band design. Its superior axial ratio bandwidth is also a result of the same broadband operation. The proposed antennas axial ratio bandwidth is also better than rest except [17]. CP gain of the proposed antenna is again comparable to rest with an almost stable value throughout the four operational bands. Most importantly, the proposed antenna employs a simple geometry with single probe feed requiring no complex feeding network like [24-26],[32], ease of fabrication through traditional low-cost techniques and attains a significantly smaller size than rest of the

reported designs. This comparison clearly shows the advantages of the proposed antenna for GNSS applications.

VI. CONCLUSION

A single-feed stacked patch antenna with quad-band operation is proposed. The simulation results are verified through experimental measurements. It has been established through the presented results that the proposed antenna works at the GPS L1, L2, L5 and 2.3 GHz frequency bands with good impedance matching and axial ratio bandwidth. The antenna has achieved good cross-polarisation ratio between RHCP/LHCP of 15 dB to mitigate interference, good circularly polarized beamwidth, a gain of more than 2.2 dBiC and efficiency of better than 70% at the four frequency bands. A detailed and systematic parametric study is carried out to understand the physics behind the antenna operation and role of the four stacked patches. It has been observed that each of the patches is independent of one another. In addition, the lower patches act as a ground plane to the subsequent patch placed above it. Therefore, it is important to ensure that the lower patch is larger in size than the upper patches.

The results have shown that the proposed antenna design offers a clear distinction between the four operating bands leading to interference mitigation, good impedance bandwidth and excellent axial ratio. It also efficiently provides concurring impedance bandwidth with axial ratio bandwidth that is one of the major challenges in CP antennas. Good circularly polarized performance, ease of design and fabrication and compact size makes the proposed antenna a potentially good candidate for small satellites, vehicles and mobile terminals.

REFERENCES

[1] Iwasaki, H. (1996). A circularly polarized small-size microstrip antenna with a cross slot. *IEEE Transaction on Antennas and Propagation*, 44(10), 1399-1401.

[2] Sharma, P. and Gupta, K.C. (1983). Analysis and optimized design of single feed circularly polarized microstrip antennas. *IEEE Transaction on Antennas and Propagation,* AP-31(6), 949-955.

[3] Geary, K.K., Schaffner, J.H., Hui-Pin, H., Song, H.J., Colburn, J.S. and Yasan, E. (2008). Single-feed dual-band stacked patch antenna for orthogonal circularly polarized GPS and SDARS applications. *Vehicular Technology Conference (VTC)*, 1-5.

[4] Falade, O.P., Ur Rehman, M., Gao, Y., Chen, X. and Parini, C.G. (2012). Single feed stacked patch circular polarized antenna for triple band GPS receivers. *IEEE Transaction on Antennas and Propagation,* 60(10), 4479-4484.

[5] Barkat, O., (2014). Modeling and optimization of radiation characteristics of triangular superconducting microstrip antenna array, *Journal of Computational Electronics*, 13(3), 657–665.

[6] Khandelwal, M.K., Kumar, S. and Kanaujia, B.K. (2018). Design, modeling and analysis of dual-feed defected ground microstrip patch antenna with wide axial ratio bandwidth. *Journal of Computational Electronics*, 17(3), 1019–1028.

[7] Chen, X., Parini, C.G., Collins, B., Yao, Y. and Ur Rehman, M. (2012). Antennas for Global Navigation Satellite Systems. *John Wiley & Sons, Ltd. (UK).*

[8] Ur Rehman, M. and Safdar, G.A. (2018). Multimode antennas for LTE femtocells in *LTE Communications and Networks: Femtocells and Antenna Design Challenges*, John Wiley & Sons, Ltd. (UK), 259-288.

[9] Rahmat-Samii Y., Noreen G.K., Dolinsky S. (1983) Spacecraft Antennas. In: Yuen J.H. (eds) Deep Space Telecommunications Systems Engineering. Applications of Communications Theory. Springer, Boston, MA.

[10] Bernhard Hofmann-Wellenhof, B., Lichtenegger, H. and Wasle, E. (2008). *GNSS – Global Navigation Satellite Systems*. Springer-Verlag Wien.

[11] Chen, Z.N. (ed)(2016), *Handbook of Antenna Technologies*, Springer, Singapore.

[12] Richards W.F. (1988) Microstrip Antennas. In: Lo Y.T., Lee S.W. (eds) *Antenna Handbook*. Springer, Boston, MA

[13] Gao, S., Brenchley, M., Unwin, M., Underwood, C.I., Clark, K., Maynard, K., Boland, L. and Sweeting, M.N. (2008). Antennas for small satellites. *Loughborough Antenna and Propagation Conference (LAPC),* 66-69.

[14] Rabemanantsoa, J. and Sharaiha, A. (2010). Size reduced dual-band printed quadrifilar helix antenna. *European Conference on Antennas and Propagation (EUCAP)*, 1–4.

[15] Hsieh, W.T., Chang, T.H. and Kiang, J.F. (2012). Dual-band circularly polarized cavity-backed annular slot antenna for GPS receiver. *IEEE Transaction on Antennas and Propagation,* 60(4), 2076–2080.

[16] Hoang, T.V., Le, T.T., Li, Q.Y. and Park, H.C. (2016). Quad-band circularly polarized antenna for 2.4/5.3/5.8-GHz WLAN and 3.5-GHz WiMAX application. *IEEE Antenna and Wireless Propagation Letters*, 15, 1032- 1035.

[17] Nasimuddin, Qing, X. and Chen, Z.N. (2014). A compact circularly polarized slotted patch antenna for GNSS applications. *IEEE Transaction on Antennas and Propagation*, 62(12), 6506–6509.

[18] Ali, T., Prasad, K.D. and Biradar, R.C. (2018). A miniaturized slotted multiband antenna for wireless applications. *Journal of Computational Electronics*,17(3), 1056–1070.

[19] Supriya, A.S and Rajendran, J. (2017). A low cost tri-band microstrip patch antenna for GPS application. *Progress in Electromagnetics Research Symposium - Fall (PIERS - FALL)*, Singapore, 60-65.
[20] Nasimuddin, Anjani, Y.S. and Alphones, A. (2015). A wide-beam circularly polarized asymmetric-microstrip antenna. *IEEE Transaction on Antennas and Propagation,* 63(8), 3764–3768.
[21] Deng, J-Y, Liu, S-Y, Sun, Dong quan, Guo, L-X, Xue, S-B. (2019). Multiband antenna for mobile terminals. *Int J RF Microw Comput Aided Eng*. 29:e21925.
[22] Fady, B, Terhzaz, J, Tribak, A, Riouch, F, Mediavilla, A. (2019). Novel miniaturized multiband antenna and applications for smart navigation media. *Int J RF Microw Comput Aided Eng*. 29:e21940.
[23] Alam, M, Mainuddin, , Kanaujia, BK, Beg, MT, Kumar, S, Rambabu, K. (2019). A hexa-band dual-sense circularly polarized antenna for WLAN/Wi-MAX/SDARS and C-band applications. *Int J RF Microw Comput Aided Eng*. 29:e21599.
[24] Tharehalli Rajanna, PK, Rudramuni, K, Kandasamy, K. (2019). Compact triband circularly polarized planar slot antenna loaded with split ring resonators. *Int J RF Microw Comput Aided Eng*. e21953.
[25] Agarwal, K., Guo, Y.X., Nasimuddin and Alphones, A. (2013). Dual-band circularly polarized stacked microstrip antenna over RIS for GPS applications. *IEEE International Wireless Symposium (IWS)*.
[26] Agarwal, K., Nasimuddin and Alphones, A. (2014). Triple-band compact circularly polarized stacked microstrip antenna over reactive impedance meta-surface for GPS applications. *IET Microwaves, Antennas and Propagation*, 8(13), 1057-1065.
[27] Schippers, H., Verpoorte, J., Jorna, P., Hulzinga, A., Thain, A., Peres, G. and Gemeren, H.V. (2009). Development of dual frequency airborne satcom antenna with optical beamforming. *IEEE Aerospace Conference,* 1-15.
[28] Chang, T.N. and Ni, G.Y. (2007). Dual band circularly polarized antenna with a quad-EMC structure. *Microwave and Optical Technology Lett*ers, 49(3), 645-647.
[29] Li, D., Guo, P., Dai, Q. and Fu, Y. (2012). Broadband capacitively coupled stacked patch antenna for GNSS applications. *IEEE Antennas and Wireless Propagation Letters*, 11, 701-704.
[30] Li, J., Shi, H., Li, H. and Zhang, A. (2014). Quad-band probe-fed stacked annular patch antenna for GNSS applications. *IEEE Antennas and Wireless Propagation Letters*, 13, 372-375.
[31] Waterhouse, R.B. (1999). Stacked patches using high and low dielectric constant material combinations. *IEEE Transaction on Antennas and Propagation,* 47(12), 1767-1771.
[32] Wang, Y., Li, Y. and Zhu, Q. (2017). A compact tri-band antenna for GPS and GSM applications. *Asia-Pacific Conference on Antennas and Propagation (APCAP)*, Xi'an, 1-3.
[33] Tsai, Y., Huang, C., Lin, C. and Hsieh, M. (2018). A dual-band dual-polarization stacked antenna array for GPS application. *Progress in Electromagnetics Research Symposium (PIERS-Toyama)*, Toyama, 2318-2323.
[34] Klionovski, K. and Shamim, A. (2017). Physically connected stacked patch antenna design with 100% bandwidth. *IEEE Antennas and Wireless Propagation Letters*, 16, 3208-3211.
[35] Li, W.T., Hei, Y.Q., Grubb, P.M., Shi, X. and Chen, R.T. (2018). Inkjet printing of wideband stacked microstrip patch array antenna on ultrathin flexible substrates. *IEEE Transactions on Components, Packaging and Manufacturing Technology*, 8(9), 1695-1701.
[36] Li, L., Huang, Y., Zhou, L. and Wang, F. (2016). Triple-band antenna with shorted annular ring for high-precision GNSS applications. *IEEE Antennas and Wireless Propagation Letters*, 15, 942-945.
[37] CST-Microwave Studio User's Manual (2019).
[38] Grewal, M.S., Andrews, A.P. and Bartone, C.G. (2013). Global Navigation Satellite Systems, Inertial navigation and integration. *John Wiley & Sons New Jersey*.
[39] Sesia, S., Toufik, I. and Baker, M. (2011). LTE – the UMTS long term evolution, from theory to practice. *Wiley & Sons Ltd*.